basis of the X-ray structure of the isoelectronic *cis*-aquabis(oxalato(2−))oxovanadate(IV).[18] These results also show that the six-coordinate geometry becomes more favorable as the bulky EHBA ligands are replaced by oxalate ligands.

Acknowledgment. The microanalysis of the samples by the Australian National University Microanalytical Service is gratefully acknowledged. P.A.L. is grateful for financial support for this project from the Australian Research Grants Scheme.

Department of Inorganic Chemistry
University of Sydney
Sydney, NSW, 2006 Australia

Rodney P. Farrell
Robert J. Judd
Peter A. Lay*

Research School of Chemistry
Australian National University
G.P.O. Box 4
Canberra, ACT, 2601 Australia

Richard Bramley*
Ji-Ying Ji

Received June 12, 1989

(18) Form, G. E.; Raper, E. S.; Oughtred, R. E.; Shearer, H. M. M. *J. Chem. Soc., Chem. Commun.* **1972**, 945–946.

Articles

Contribution from the Department of Chemistry, University of Michigan, Ann Arbor, Michigan 48109-1055

Stepwise, Metal-Assisted Decarboxylation Promoted by Manganese: Reactivity Relationship between Manganese and Vanadium

Xinhua Li and Vincent L. Pecoraro*

Received November 2, 1988

Manganese(III) complexes of the ligand ethylenebis[(*o*-hydroxyphenyl)glycine], $Mn(EHPG)^-$, are shown to oxidatively decarboxylate in methanol, DMF, and acetone solutions to generate derivatives of [ethylenebis(salicylideneaminato)]manganese(III), $Mn(SALEN)^+$. This process occurs via air oxidation of $Mn^{III}(EHPG)^-$ to form $Mn^{IV}(EHPG)$, which subsequently loses CO_2 and one proton, forming [*N*-(2-(*o*-salicylideneamino)ethyl)(*o*-hydroxyphenyl)glycinato]manganese(III), $Mn^{III}(EHGS)$. $Mn^{III}(EHGS)$ is also air sensitive and will further decarboxylate to $Mn^{III}(SALEN)^+$. When this reaction is completed in acetone, X-ray-quality crystals of $Mn^{III}(SALEN)$[2-(3-oxobutenyl)phenolate] are recovered. This very loosely associated solid-state dimer contains a rare example of monodentate phenolate coordination to Mn(III). The generation of $Mn^{III}(SALEN)^+$ has been followed by electrochemistry and paramagnetic NMR spectroscopy. $Mn^{III}(EHPG)^-$ shows an oxidative wave in methanol with $E_0 = +450$ mV and in DMF with $E_0 = +300$ mV (vs SCE). Bulk electrolysis at +600 mV in methanol quantitatively (by the passage of four electrons) generates $Mn^{III}(SALEN)^+$, which has an Mn(III)/Mn(II) reduction at −250 mV. The paramagnetic NMR spectrum of a mixture of *rac* and *meso* isomers of $Mn^{III}(EHPG)^-$ in CD_3OD shows resonances at +26.3, −18.6, and −34.6 ppm (*rac* isomer) and +27.8, +24.0, −2.4, −16.5, −22.5, −32.5, and −35.5 ppm (*meso* isomers). After 9 days, the spectrum of $Mn^{III}(SALEN)^+$ has developed completely with resonances at −4.1, −23.2, and −28.9 ppm. $Mn^{III}(EHGS)$ is not produced in sufficient quantities to be detected under these conditions. In contrast, DMF solutions of $Mn^{III}(EHPG)^-$ (shifts at +27.3, +24.8, −2.4, −18.0, −21.6, −32.0, and −35.5 ppm, *meso* isomer) slowly form $Mn^{III}(EHGS)$ with features at +45.6, +28.6, +13.1, −9.4, −19.5, and −27.7 ppm, and ultimately one recovers $Mn^{III}(SALEN)^+$ with peaks at +29.5, −2.4, −22.3, and −25.4 ppm. In contrast, the $Fe^{III}(EHPG)^-$, $Cu^{II}(EHPG)^{2-}$, and $Ga^{III}(EHPG)^-$ complexes are air stable. This metal-assisted, oxidative decarboxylation is analogous to that previously described for $V^VO(HEHPG)$, which was shown to generate V(III) species as intermediates. Therefore, this facile decarboxylation reaction appears to be promoted by using ions that can cycle through three oxidation states and suggests that a cycle for the manganese-facilitated process includes both Mn(IV) and Mn(II). X-ray parameters for $Mn^{III}(SALEN)$[2-(3-oxobutenyl)phenolate]: $MnC_{26}H_{23}N_2O_4$, mol wt 482.4, monoclinic ($P2_1/c$), $a = 12.200$ (4) Å, $b = 14.104$ (4) Å, $c = 13.584$ (3) Å, $\beta = 103.74$ (2)°, $V = 2270$ (1) Å^3, $Z = 4$, 3503 unique data collected with $0 < 2\theta < 45°$, 1708 data with $I > 3\sigma(I)$. The best model gave $R = 0.044$ and $R_w = 0.039$.

Introduction

The biological chemistry of manganese is garnering considerable attention due to the recent demonstration of this element as an important cofactor in the generation[1] and metabolism[2,3] of O_2^{n-} (where $n = 0$–2). A mononuclear metal center has been established[4] for manganese superoxide dismutase. The manganese catalases of *Thermus thermophilus*[2c,d] and *Lactobacillus plantarum*[2e] apparently have dinuclear active centers. One proposal for the metal nuclearity of the oxygen-evolving complex[5] includes a mononuclear component, although there is considerable controversy in this area.[1,6]

The structure and reactivity relationship between iron and manganese, and its importance to biological properties of these elements, has been established for some time. Iron complexes have

(1) Recent reviews of this subject include: (a) Pecoraro, V. L. *Photochem. Photobiol.* **1988**, *48*, 249. (b) Babcock, G. T. In *Comprehensive Biochemistry: Photosynthesis*; Amesz, J., Ed.; Elsevier-North Holland: Amsterdam, 1987; Vol. 15, p 121. (c) Amesz, J. *Biochim. Biophys. Acta* **1983**, *726*, 1. (d) Dismukes, G. C. *Photochem. Photobiol.* **1986**, *43*, 99.

(2) (a) Beyer, W. F., Jr.; Fridovich, I. *Biochemistry* **1985**, *24*, 6460. (b) Kono, Y.; Fridovich, I. *J. Biol. Chem.* **1983**, *258*, 13646. (c) Khangulov, S. V.; Barynin, V. R.; Melik-Adamyin, V. R.; Grebenko, A. I.; Voevodskaya, N. V.; Blumenfeld, L. A.; Dobryakov, S. N.; Il'Yasova, V. B. *Bioorg. Khim.* **1986**, *12*, 741. (d) Barynin, V. R.; Vagin, A. A.; Melik-Adamyin, V. R.; Grebenko, A. I.; Khangulov, S. V.; Popov, A. N.; Anrianova, M. E.; Vainshtein, B. K. *Sov. Phys.—Dokl.* (*Engl. Transl.*) **1986**, *31*, 457. (e) Fronco, R. M.; Penner-Hahn, J. E.; Bender, C. J. *J. Am. Chem. Soc.* **1988**, *110*, 7554.

(3) Ludwig, M. L.; Pattridge, K. A.; Stallings, W. C. *Manganese in Metabolism and Enzyme Function*; Adacemic Press: New York, 1986; p 405.

(4) Stallings, W. C.; Pattridge, K. A.; Strong, R. K.; Ludwig, M. L. *J. Biol. Chem.* **1985**, *260*, 16424.

(5) Hansson, O.; Aasa, R.; Vanngard, T. *Biophys. J.* **1987**, *51*, 825.

(6) dePaula, J. C.; Beck, W. F.; Brudvig, G. W. *J. Am. Chem. Soc.* **1986**, *108*, 4002.

0020-1669/89/1328-3403$01.50/0

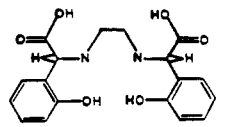

H_4EHPG

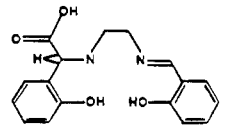

H_3EHGS

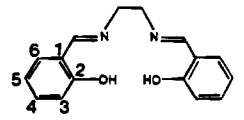

H_2SALEN

Figure 1. Ligands used or generated in this study.

been used successfully to predict reasonable synthetic targets for manganese materials.[7] The serum iron transport protein transferrin will also bind Mn(III) with high affinity.[8] In addition, a reactivity relationship between manganese and iron is often observed. Manganese porphyrin complexes have provided considerable insight for defining the chemical mechanism of heme enzymes such as cytochrome P_{450}.[9] Thus, mononuclear manganese and iron complexes that are involved in two-electron, oxo-group-transfer chemistry[9,10] (usually cycling between Mn(II) and Mn(IV), Fe(II) and Fe(IV), or Fe(III) and Fe(V)) often behave similarly. Furthermore, one-electron transformations are observed for both iron and manganese superoxide dismutases.[3]

While the iron/manganese relationship has often proved quite fertile, there are cases where it breaks down. The generation of high-valent iron often requires special ligands such as porphyrins or Schiff bases, while Mn(IV) compounds are obtained with a variety of coordination environments.[11-15] Therefore, two-electron chemical transformations facilitated by manganese, but not iron, are possible. In this report, we examine whether the reactivity properties of vanadium may, in certain instances, provide better insight into the reactivity of mononuclear manganese coordination compounds than the analogous iron complex.

Vanadium is known[16,17] to facilitate the oxidative decarboxylation of the polyamino carboxylic acid ligands H_4EHPG and H_3EHGS, shown in Figure 1, to generate VO(SALEN). In contrast, $[Fe(EHPG)]^-$ and $[Fe(EHGS)(CH_3OH)]$ are very stable and have been characterized by X-ray analysis.[18,19] We have investigated the chemistry of manganese with H_4EHPG and E_3EHGS and report herein that manganese is competent to carry out this two-electron oxidative decarboxylation to generate Mn(SALEN)X, where X may be a number of monodentate anions. We have followed the reaction by using electrochemistry and the paramagnetically shifted proton resonances of the phenolate ligands in a variety of solvents. One product, Mn(SALEN)[2-(3-oxobutenyl)phenolate], is shown by an X-ray analysis to contain a rare example of monodentate phenolate coordination to Mn(III). This contribution thereby establishes a potential reactivity analogy for mononuclear, high-valent manganese and vanadium coordination complexes via two-electron chemistry using ligand environments that are more similar to those proposed for manganese enzymes than obtained with the porphyrin molecule.

Experimental Section

Abbreviations: H_2SALEN = *N,N'*-disalicylideneethylenediamine; H_4EHPG = ethylenebis[(*o*-hydroxyphenyl)glycine]; H_3EHGS = *N*-(2-(*o*-salicylideneamino)ethyl)(*o*-hydroxyphenyl)glycine.

Materials. H_4EHPG was purchased from Aldrich Chemical Co. Tetrabutylammonium hexafluorophosphate ($(TBA)PF_6$) was made by the metathesis of tetrabutylammonium bromide and ammonium hexafluorophosphate in water and recrystallized from hot ethanol prior to electrochemical studies. High-purity solvents for electrochemical studies were purchased from American Burdick and Jackson Co. and used as received. These solvents were stored under nitrogen. High-purity argon gas was used to deaerate solutions. All other chemicals and solvents were reagent grade. Elemental analyses were performed by Galbraith Analytical Laboratories, Inc., Knoxville, TN.

Synthesis of Compounds. *meso*-Na[Mn(EHPG)]·3H$_2$O (1). *meso*-$Mn(EHPG)^-$ was prepared by taking 1.8 g (5.0 mmol) of H_4EHPG and 0.8 g (20 mmol) of NaOH and dissolving them in degassed methanol (20 mL) maintained under nitrogen. After 5 min of stirring, all of the H_4EHPG had dissolved, giving a clear, red solution. At this point, 20 mL of a methanol solution containing 1.34 g (5.0 mmol) of $Mn(OAc)_3\cdot 2H_2O$ was added to give a brown solution. After 20 min of stirring, 30 mL of acetonitrile was added and a brown solid precipitated, was recovered by filtration on a Schlenk line, and then dried in air. The yield of *meso*-$Na[Mn(EHPG)]\cdot 3H_2O$ was ~80%. *meso*-H_4EHPG was isolated by demetalation of this product. *meso*-NaMnEHPG was reacted with an extra amount of 8-hydroxyquinoline in MeOH. After 2 h of stirring, tris(8-hydroxyquinolinato)manganese precipitated as a brown solid. The filtrate was flash-evaporated to dryness. Chloroform was used to extract the residue, and water was added to $CHCl_3$ in a separatory funnel. The aqueous layer was washed with $CHCl_3$ until there was no more 8-hydroxyquinoline present. The pH of the aqueous phase was adjusted to about 6, and *meso*-H_4EHPG was precipitated and obtained by filtration.

***rac*-Na[Mn(EHPG)]·3H$_2$O (2).** The *rac* isomer of H_4EHPG was obtained by the selective decarboxylation of *meso*-VO(HEHPG) from the original mixture of isomers present in methanol.[17] Under these conditions, the *rac*-VO(HEHPG) isomer does not decarboxylate; instead, it forms *rac*-VO_2EHPG^{3-}, which can be separated from $VO(EHGS)^-$ by fractional crystallization. *rac*-H_4EHPG can then be obtained by demetalation of an aqueous solution of *rac*-VO_2EHPG^{3-} with use of acid. Under these conditions, the pure ligand precipitates immediately from solution. The *rac* isomer of $Mn(EHPG)^-$ was prepared as described above by using the resolved *rac*-H_4EHPG as starting material. Anal. Calcd for $Na[Mn(EHPG)]\cdot 3H_2O$ (mol wt = 488): C, 44.26; H, 4.51; N, 5.74; Mn, 11.27. Found: C, 44.01; H, 4.12; N, 5.14; Mn, 11.90.

TBA[Ga(EHPG)] (3) and Mg[Ga(EHPG)]$_2$ (4). $Mg[Ga(EHPG)]_2$ was synthesized and isolated by following published procedures.[21] All physical properties of the isolated solid were consistent with those of authentic $Mg[Ga(EHPG)]_2$. TBA[Ga(EHPG)] was prepared by using tetrabutylammonium hydroxide ((TBA)OH) as a base instead of $MgCO_3$. $(TBA)_4EHPG$ was prepared in situ by the addition of (TBA)OH to a DMF solution of H_4EHPG in order to solubilize the free-acid form of the ligand.

Mn(SALEN)X (X = 2-(3-Oxobutenyl)phenolate (5), Acetate (6), Chloride (7)). Five millimoles (1.8 g) of H_4EHPG and 20 mmol (13 mL) of tetrabutylammonium hydroxide (40% solution in MeOH) were added to a degassed mixture of 50 mL of methanol and 50 mL of water. After a clear solution was obtained, 5 mmol (1.34 g) of $Mn(OAc)_3\cdot 2H_2O$ was added. This brown solution was stirred for 3 h under nitrogen and then opened to the air and stirred for an additional 12 h. The solution was flash-evaporated, and the residue was redissolved in acetone. X-ray-

(7) Sheats, J. E.; Czernuszewicz, R. S.; Dismukes, G. C.; Rheingold, A. L.; Petroleas, V.; Stubbe, J.; Armstrong, W. H.; Beer, R. H.; Lippard, S. J. *J. Am. Chem. Soc.* **1987**, *109*, 1435.
(8) O'Hara, P.; Yeh, S. M.; Meares, C. F.; Bersohn, R. *Biochemistry* **1981**, *20*, 4704.
(9) Groves, J. T.; Stern, M. K. *J. Am. Chem. Soc.* **1987**, *109*, 3812.
(10) Srinivasan, K. P.; Michaud, P.; Kochi, J. K. *J. Am. Chem. Soc.* **1986**, *108*, 2309.
(11) Kessissoglou, D. P.; Li, X.; Butler, W. M.; Pecoraro, V. L. *Inorg. Chem.* **1987**, *26*, 2487.
(12) Hartmann, J. R.; Foxman, B. M.; Cooper, S. R. *Inorg. Chem.* **1984**, *23*, 1381.
(13) Pavacik, P. S.; Huffman, J. C.; Christou, G. *J. Chem. Soc., Chem. Commun.* **1986**, 43.
(14) Chin, D.; Sawyer, D. T.; Schaefer, W. P. *Inorg. Chem.* **1983**, *22*, 752.
(15) Koikawa, M.; Okawa, H.; Kida, S. *J. Chem. Soc., Dalton Trans.* **1988**, 641.
(16) Pecoraro, V. L.; Bonadies, J. A.; Marese, C. A.; Carrano, C. J. *J. Am. Chem. Soc.* **1984**, *106*, 3360.
(17) Bonadies, J. A.; Carrano, C. J. *J. Am. Chem. Soc.* **1986**, *108*, 4088.
(18) Bailey, N. A.; Cummings, D.; McKenzie, E. D.; Worthington, J. M. *Inorg. Chim. Acta* **1981**, *50*, 111.
(19) Carrano, C. J.; Spartalian, K.; Appa Rao, G. V. N.; Pecoraro, V. L.; Sundaralingam, M. *J. Am. Chem. Soc.* **1985**, *107*, 1651.
(20) Patch, M. G.; Simolo, K. P.; Carrano, C. J. *Inorg. Chem.* **1982**, *21*, 2972.
(21) Riley, P. E.; Pecoraro, V. L.; Carrano, C. J.; Raymond, K. N. *Inorg. Chem.* **1983**, *22*, 3096.

Table I. Summary of Crystal Data for Mn(SALEN)[2-(3-oxobutenyl)phenolate]

formula	$MnC_{26}H_{23}N_2O_4$
mol wt	482.4
a, Å	12.200 (4)
b, Å	14.104 (4)
c, Å	13.584 (3)
β, deg	103.74 (2)
V, Å^3	2270 (1)
cryst syst	monoclinic
space group	$P2_1/c$
d_{calc}, g/mL	1.41
d_{obs}, g/mL	1.40
Z	4
radiation	Mo Kα (0.7107 Å)
abs coeff, m, cm^{-1}	5.61
temp, K	298
cryst size, mm	0.11 × 0.36 × 0.37
scan speed, deg/min	2.5–12
scan range, deg	$0 < 2\theta < 45$
bdgd/scan time ratio	0.8
no. of unique data collected	3503
no. of obs data ($I > 3\sigma(I)$)	1708
largest non-solv residual	0.28
R	0.044
R_w	0.039
GOF	1.43

quality crystals were obtained from the slow evaporation of acetone solution. If DMF or acetonitrile was used as the solvent for recrystallization, a polymeric Mn^{III}SALEN(OAc)[22] was recovered. Mn(SALEN)Cl[23] was formed when $MnCl_2$ was the source of metal. The yield of Mn(SALEN)(OAc) was 60% and for Mn(SALEN)[2-(3-oxobutenyl)phenolate] was 40% based on manganese. The latter material is somewhat hygroscopic. Anal. Calcd for Mn(SALEN)[2-(3-oxobutenyl)phenolate]·$2H_2O$ ($C_{26}H_{27}N_2O_6Mn$, mol wt = 518): C, 60.23; H, 5.21; N, 5.41; Mn, 11.62. Found: C, 59.55; H, 5.43; N, 5.45; Mn, 11.91.

Collection and Reduction of X-ray Data. Suitable crystals of Mn(SALEN)[2-(3-oxobutenyl)phenolate] (**5**) were obtained as described above and mounted in glass capillaries. Intensity data were obtained at room temperature on a Syntex $P2_1$ diffractometer using Mo Kα radiation (0.7107 Å) monochromatized by a graphite crystal whose diffraction vector was parallel to the diffraction vector of the sample. Three standard reflections were measured every 50 reflections. The crystal and data parameters are given in Table I. Intensity data were collected by using $\theta/2\theta$ scans. Crystal faces were measured, and a numerical absorption correction was applied to the data set. The data were reduced by using the SHELX76 program package,[24] and the structure was solved by using SHELX86. The SHELX76 program was used for subsequent refinement of the model. Computations were carried out on an Amdahl 5860 computer. Atomic scattering factors used were from ref 25. Hydrogen atoms were located but not refined and placed at fixed distances from bonded carbon atoms of 0.95 Å in the final difference map. Unique data and final R indices are reported in Table I. Fractional atomic coordinates are reported in Table II, and a selected list of bond lengths and angles is given in Table III.

Electrochemical Measurements. Cyclic and rotating-platinum-electrode voltammetries and bulk electrolyses were completed at 23 ± 2 °C with a BAS-100 electrochemical analyzer. Cyclic voltammograms were generated by using a three-electrode system composed of platinum-bead, platinum-wire, and saturated calomel (SCE, within a Luggin probe) electrodes as the working, auxiliary, and reference electrodes, respectively. Bulk electrolyses utilized either a platinum basket or a platinum screen for working and auxiliary electrodes, each being separated by a fine frit. (TBA)PF_6 was used as the supporting electrolyte at 0.1 M concentration. All potentials are referenced versus the ferrocene/ferrocenium couple employed as an external reference.

Spectroscopic and Magnetic Measurements. UV/vis spectra were recorded on a Perkin-Elmer Lambda 9 UV/vis/near-IR spectrophotometer equipped with a Perkin-Elmer 3600 data station. Infrared spectra were recorded on a Nicolet 60 SX Fourier transform spectrometer with samples prepared as KBr pellets. NMR spectra were obtained on a Bruker 360-MHz FT-NMR spectrometer operating in the quadrature detection mode. Spectra were collected by using a one-pulse sequence with a 90° pulse of 9.9 μs. Between 3000 and 10 000 transients were accumulated over a 50-kHz bandwidth for each sample, with each spectrum containing 8K data points. Spectra were referenced to the primary solvent peak in the diamagnetic region and are reported versus $(CH_3)_4Si$ as 0 ppm. A spline fit routine was utilized for base-line correction. Solid-state magnetic moments were determined with a Johnson-Matthey magnetic susceptibility balance (MSB-1) using Hg[Co(SCN)$_4$] as a calibration standard. Magnetic moments for solution species were obtained by using the Evans NMR procedure.[26,27]

EHPG Isomer Identification. The identity of the EHPG ligand isomer (*rac* or *meso*) in the metal complexes[28] was determined by either of two methods. The first is based on the TLC behavior of the FeEHPG$^-$ complexes prepared by the reaction of ferric chloride and H_4EHPG ligand (mixed, *rac* or *meso*). The chromatogram of the resulting iron complexes shows two spots for a mixture of isomers, one spot (R_f 0.14) for *meso* and one spot (R_f 0.37) for *rac* isomers on silica gel plates using

Table II. Fractional Atomic Coordinates for Mn(SALEN)[2-(3-oxobutenyl)phenolate]

atom	x	y	z	U_{eq}, Å^2
Mn1	0.5164 (2)	0.1166 (1)	0.4477 (1)	0.041
O1	0.4176 (7)	0.0795 (6)	0.3244 (6)	0.045
O2	0.6098 (8)	0.0096 (6)	0.4519 (6)	0.048
O3	0.6019 (9)	0.2168 (6)	0.3916 (6)	0.056
N1	0.4071 (9)	0.2110 (7)	0.4731 (8)	0.043
N2	0.5873 (10)	0.1414 (7)	0.5928 (7)	0.041
C1	0.3215 (11)	0.1196 (10)	0.2747 (9)	0.041
C2	0.2703 (12)	0.1955 (10)	0.3134 (10)	0.042
C3	0.1692 (12)	0.2334 (10)	0.2542 (11)	0.056
C4	0.1192 (13)	0.1975 (12)	0.1595 (12)	0.066
C5	0.1701 (13)	0.1206 (13)	0.1234 (9)	0.060
C6	0.2685 (12)	0.0820 (9)	0.1788 (9)	0.049
C7	0.3134 (13)	0.2344 (9)	0.4114 (11)	0.047
C8	0.4462 (13)	0.2618 (10)	0.5712 (11)	0.063
C9	0.5129 (12)	0.1929 (10)	0.6446 (10)	0.058
C10	0.6869 (13)	0.1139 (10)	0.6393 (10)	0.045
C11	0.7584 (12)	0.0548 (10)	0.5961 (10)	0.044
C12	0.8706 (13)	0.0409 (10)	0.6509 (10)	0.059
C13	0.9394 (13)	−0.0201 (12)	0.6177 (13)	0.069
C14	0.8986 (14)	−0.0701 (11)	0.5278 (13)	0.066
C15	0.7901 (13)	−0.0581 (10)	0.4723 (10)	0.054
C16	0.7173 (12)	0.0036 (10)	0.5050 (10)	0.044
C17	0.7054 (13)	0.2431 (10)	0.3941 (9)	0.044
C18	0.7709 (13)	0.1991 (10)	0.3325 (10)	0.045
C19	0.8789 (14)	0.2343 (12)	0.3362 (11)	0.063
C20	0.9231 (13)	0.3094 (12)	0.3955 (13)	0.068
C21	0.8588 (16)	0.3522 (10)	0.4549 (11)	0.065
C22	0.7532 (14)	0.3194 (11)	0.4552 (10)	0.056
C23	0.7182 (13)	0.1206 (11)	0.2690 (10)	0.061
C24	0.7576 (15)	0.0730 (12)	0.2027 (12)	0.072
C25	0.6980 (21)	−0.0061 (12)	0.1405 (12)	0.092
C26	0.5831 (20)	−0.0361 (12)	0.1492 (11)	0.106
O4	0.7424 (15)	−0.0472 (8)	0.0823 (10)	0.157

[a] $U_{eq} = {}^1/_3\sum_i\sum_j U_{ij}a^*_i\alpha^*_i\vec{a}_i\vec{a}_j$.

Table III. Selected Bond Lengths (Å) and Angles (deg) for Mn(SALEN)[2-(3-oxobutenyl)phenolate]

Mn1–O1	1.892 (4)	Mn1–N1	1.973 (5)
Mn1–O2	1.886 (4)	Mn1–N2	1.991 (4)
Mn1–O3	2.012 (4)	Mn1–Mn1′	3.644 (2)
Mn1′–O2	2.897 (4)		
O1–Mn1–O2	93.6 (2)	O1–Mn1–O3	98.1 (2)
O1–Mn1–N1	91.4 (2)	O1–Mn1–N2	164.4 (2)
O2–Mn1–O3	102.0 (2)	O2–Mn1–N1	164.7 (2)
O2–Mn1–N2	89.5 (2)	O3–Mnu–N1	91.6 (2)
O3–Mn1–N2	96.2 (2)	N1–Mn1–N2	82.0 (2)

(22) Davies, J. E.; Gatehouse, B. M.; Murray, K. S. *J. Chem. Soc., Dalton Trans.* **1973**, 2523.
(23) Pecoraro, V. L.; Butler, W. M. *Acta Crystallogr.* **1985**, *C42*, 1151.
(24) Sheldrick, G. Institut for Anorganische Chemie der Universitat Gottingen, Gottingen, Federal Republic of Germany. Other programs include ORTEP, a thermal ellipsoidal drawing program by C. K. Johnson.
(25) *International Tables for X-ray Crystallography*; Ibers, J., Hamilton, W., Eds.; Kynoch: Birmingham, England, 1974; Vol. IV, Tables 2.2 and 2.3.1.
(26) Bartle, K. D.; Dale, B. J.; Jones, D. W.; Maricic, J. *J. Magn. Reson.* **1973**, *12*, 286.
(27) Evans, D. F. *J. Chem. Soc.* **1959**, 2003.
(28) *meso*-EHPG forms *meso*-Mn(EHPG)$^-$, and *rac*-EHPG forms *rac*-Mn(EHPG)$^-$.

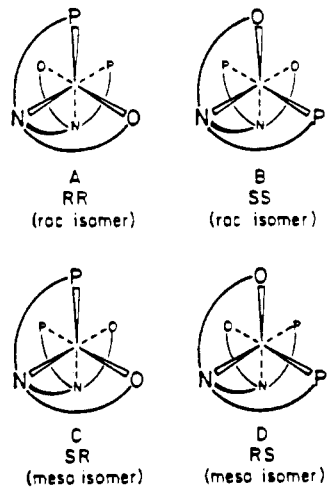

Figure 2. Four of the possible absolute stereochemical isomers that can be formed in octahedral metal complexes of EHPG. The top two isomers are formed by the *rac* form of EHPG (*RR* or *SS*), while the bottom two isomers are the *meso* form of EHPG (*RS* or *SR*). All of the isomers have the Λ screw sense configuration. The Δ isomers are mirror-related to those shown (e.g., the mirror relative of A is Δ-*SS*). The figure was taken from ref 21.

5:3:0.3 EtOH/toluene/MeOH as the eluting solvent. The second method of distinguishing the ligand isomers is via the proton NMR spectra of the free ligands. The ligand was dissolved in D_2O at pH = 10.5. The internal standard was the sodium salt of 3-(trimethylsilyl)-1-propanesulfonic acid (0.0 ppm). The protons on the chiral carbons shift in a characteristic fashion for each of the two forms (*rac*, 4.38 ppm; *meso*, 4.45 ppm) and can be identified by this method. The chemical shifts of these peaks are seen to vary as a function of pH.[17]

Results and Discussion

Evidence for Oxidative Chemistry. The reaction of $Mn(OAc)_3$ with Na_4EHPG in methanol/acetonitrile generates the red-brown complex Na[Mn(EHPG)]. A slow oxidative decarboxylation is observed when Na[Mn(EHPG)] (both *meso* and *rac* isomers) is dissolved in methanol, DMF, or acetone without exclusion of atmospheric oxygen. In methanol, the recovered product is an infinite chain of Mn(SALEN)OAc, the structure of which has previously been described.[22] In acetone, the reaction again goes to completion, this time generating Mn(SALEN)[2-(3-oxobutenyl)phenolate], which is described below. The axial phenolate is the product of an aldol condensation between salicylaldehyde and acetone. Similarly, in DMF, $Mn(SALEN)^+$ can be recovered after exposure to atmospheric oxygen for 1 week. The solid $Mn(EHPG)^-$ also decarboxylates when exposed to air for 1–2 months. This reactivity is very similar to that observed for VO(HEHPG) but is entirely different from the behavior of $Fe(EHPG)^-$, $Ga(EHPG)^-$, $Cu(EHPG)^{2-}$, and $Co(EHPG)^-$. In the latter cases, solids that are stable indefinitely are recovered.

Structural Descriptions of *meso*-$Mn(EHPG)^-$, *rac*-$Mn(EHPG)^-$, and Mn(SALEN)[2-(3-oxobutenyl)phenolate]. In order to define the metal chelate stereochemistry, we have followed the description of Riley et al.,[21] who have provided a detailed stereochemical analysis of six-coordinate metallo EHPG complexes. The H_4EHPG ligand is an amino acid derivative and, as such, has diastereomers since there are two chiral carbon atoms. Thus, one obtains both *meso* (*RS* and *SR*) and *rac* (*RR* and *SS*) isomers. In the metal complex, the carboxylate, phenolate, and nitrogen atoms that are bonded to a specific chiral center are required to occupy mutually cis positions, forming a face of the metal octahedron. The same ligating atoms associated with the other chiral atom form the remaining trigonal face. The axis that is normal to these faces is chosen as the reference axis. This view is shown in Figure 2.[21] With O and P defined as carboxylate and phenolate oxygen atoms, respectively, Figure 2 shows four possible stereochemical arrangements. The number of available isomers is severely restricted because the two nitrogen atoms are also constrained into cis positions. Fixing the nitrogen into the left corner of the top trigonal face restricts the two possible orientations with respect to the reference axis, specified as a right-handed (counterclockwise) rotation, as NOP or NPO. The chirality of the carbon atom determines the sequence of the ligating groups on this face. A similar situation holds for the bottom face. For *rac*-EHPG with the *RR* configuration, structure A is generated by an NOP orientation on the top face and an NPO orientation on the bottom face. By using the reference axis defined above, and by examining all of the skew chelate pairs that lie along the edges of the pseudooctahedral coordination polyhedron,[21,29] we can define Λ and Δ absolute configurational isomers. Thus, structures A–D are designated Λ-*RR*, Λ-*SS*, Λ-*SR*, and Λ-*RS*, respectively.

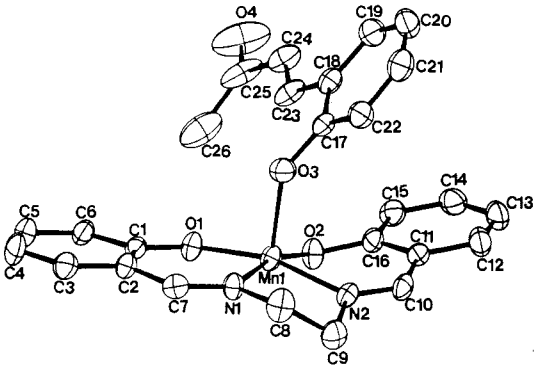

Figure 3. ORTEP diagram of Mn(SALEN)[2-(3-oxobutenyl)phenolate], with the atom-numbering scheme and thermal ellipsoids given at 30% probability.

It has been shown previously[21] that the Λ-*RR* and Δ-*SS* isomers are the preferred forms of *rac*-M(EHPG) structures. Indeed, every structurally examined *rac*-M(EHPG) species has crystallized in the Λ-*RR* (Δ-*SS*) form. In this geometry, the two carboxylate groups are positioned trans to one another. This contrasts with the most stable[18,21,30,31] *meso* isomers (C, Λ-*SR* (Δ-*RS*); D, Λ-*RS* (Δ-*SR*)), which have phenolates and carboxylates in cis positions. For these reasons, we believe that *rac*-$Mn(EHPG)^-$ is isostrucural with the previously described[21] Λ-(*RR*)-$Cu(EHPG)^{2-}$. Both Cu^{2+} (d^9) and Mn^{3+} (high-spin d^4) complexes are usually Jahn–Teller-distorted with a 0.2–0.3-Å elongation of chemically equivalent bonds along the *z* axis relative to the tetragonal plane. In fact, $Cu(EHPG)^{2-}$ shows average $Cu-O_{phenolate}$ and average $Cu-O_{carboxylate}$ bond lengths of 1.94 and 2.43 Å, respectively. The trans carboxylate configuration, which places the six-membered imino phenolate chelate rings in the tetragonal plane, should be a very stable configuration for Mn(III), while the *meso* isomers (Λ-*SR* (Δ-*RS*) and Λ-*RS* (Δ-*SR*)) are more highly strained, as an elongation along any molecular direction will require one of these rigid, six-membered imino phenolate rings to span the distorted axis.

An ORTEP diagram of the product of the $Mn(EHPG)^-$ decarboxylation, Mn(SALEN)[2-(3-oxobutenyl)phenolate], is given in Figure 3, and important bond lengths and angles are provided in Table III. The manganese coordination sphere is very similar to that observed[23] for Mn(SALEN)Cl. The tetragonal plane is composed of O1, O2, N1, and N2 at typical distances for Mn(III).[1a,23] The axial position is filled by the 2-(3-oxobutenyl)-phenolate anion at a long 2.012 Å. This is the first example of a structurally characterized complex in which a monodentate phenolate is coordinated to manganese(III), although an axial monodentate thiophenolate complex has recently been reported.[32] The manganese ion is displaced out of the best least-squares plane toward the axial anion by 0.24 Å. Thus, the polyhedron described is square pyramidal. One could also view the complex as a very weakly associated solid-state dimer in which phenolates O2 and

(29) The IUPAC nomenclature for octahedral complexes containing five- and six-membered chelate rings is given in: *Inorg. Chem.* **1970**, *9*, 1.
(30) Bernauer, K. *Top. Curr. Chem.* **1976**, *65*, 1.
(31) Bailey, N. A.; Cummings, D.; McKenzie, E. D.; Worthington, J. M. *Inorg. Chim. Acta* **1976**, *18*, L3.
(32) Gohdes, J. W.; Armstrong, W. H. *Inorg. Chem.* **1988**, *27*, 1841.

Table IV. Electrochemical Parameters[a] for Mn(EHPG)$^-$ and Related Complexes

compd	solvent	E_a	E_c	ΔE	i_a[b]	i_c[b]	i_a/i_c
Mn(EHPG)$^-$	MeOH	+491	+416	75	0.61	0.20	2.98
Mn(EHPG)$^-$	DMF	+369	+230	139	0.70	0.32	2.1
Mn(SALEN)$^+$	MeOH	−202	−291	89	1.1	1.2	0.92
Mn(SALEN)$^+$	DMF	−188	−271	86	3.9	6.2	0.63
Ga(EHPG)$^-$	DMF	+1038	...	...	3.2	...	...
$[N(Bu_4)]_4$EHPG	DMF	+760	...	...	0.8	...	...
VO(EHPG)$^{2-}$	MeOH	+310[c]					
VO(EHPG)$^{2-}$	DMF	+176[c]					
VO(EHGS)$^-$	MeOH	+134[c]					
VO(EHGS)$^-$	DMF	+20[c]					
VO(SALEN)	MeOH	+300[c]					
VO(SALEN)	DMF	+375[c]					

[a] All potentials reported in millivolts versus the standard calomel electrode (SCE) referenced against an external ferrocene/ferrocenium couple; scan rate 100 mV/s. [b] Currents (A) reported are multiplied by 10^5. [c] $E°$ for V(IV)/V(V) couple reported in ref 17.

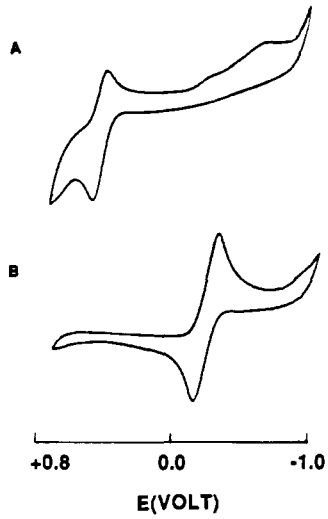

Figure 4. Cyclic voltammogram of Mn(EHPG)$^-$ in methanol (A) before electrolysis at +600 mV and (B) after the electrolysis.

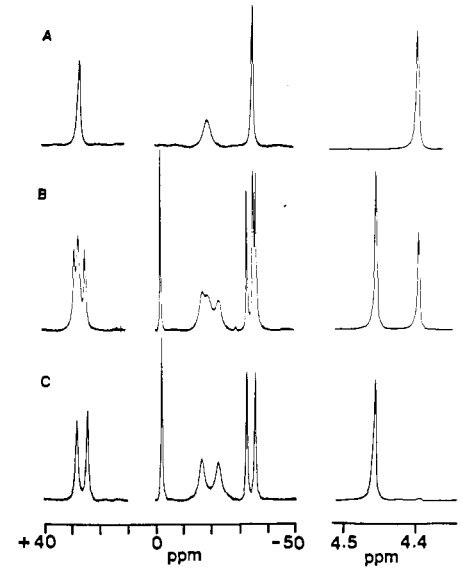

Figure 5. ^{1}H NMR spectra of approximately 10 mM *meso*-Mn(EHPG)$^-$ solutions in methanol-d_4 (at left) and the uncomplexed ligand EHPG in D_2O: (A) *rac*-Mn(EHPG)$^-$; (B) ~50:50 mixture of *rac*- and *meso*-Mn(EHPG)$^-$; (C) *meso*-Mn(EHPG)$^-$. The ligand spectra at right show the amounts of *rac* (+4.38 ppm) and *meso* (+4.45 ppm) isomers recovered from each sample.

O2′ (related through an inversion center) bridge the metal centers. The manganese–manganese separation is 3.644 Å, and the Mn1–O2 distance is a very long 2.897 Å. This Mn–Mn separation is comparable to that observed (~3.5 Å) in trinuclear alkoxy/acetate-bridged systems[33,34] but is much longer than that seen for other diphenolate-bridged Mn^{II}_2 (3.3 Å)[35] or Mn^{III}_2 (3.25 Å)[36] dimers. The metal separation in Mn(SALEN)Cl[23] is 3.46 Å, and the closest metal separation in the mononuclear Mn(SALEN)(*p*-nitrobenzenethiolate)[32] is 4.14 Å. This weak interaction may be important in the solid-state chemistry of the Mn(SALEN)X family;[37] however, in solution Mn(SALEN)$^+$ is the sole chemical species.

Electrochemistry of Compounds. We have carried out an electrochemical study of the Mn(III) polyamino carboxylate complexes in order to establish the accessibility of the Mn(IV) oxidation state and the potential importance of this oxidation level to the observed ligand decarboxylation reactions. A summary of the electrochemical parameters for Mn(EHPG)$^-$ and related complexes is given in Table IV. A quasi-reversible, one-electron oxidation of Mn(EHPG)$^-$ is centered at +454 mV (versus SCE) in methanol (Figure 4). That this wave is an oxidation is confirmed by rotating-platinum-electrode voltammetry (RPE).[38] This oxidation shifts to +300 mV in DMF.

If oxygen is admitted to a methanol solution of Mn(EHPG)$^-$ and the reaction mixture allowed to stand for 1 week, a new, nearly reversible reductive wave at −247 mV is observed. This electrochemistry is identical with the reductive behavior of Mn(SALEN)$^+$ in methanol. Examination of solutions that were 1 and 4 days old provided no evidence for the generation of an intermediate species corresponding to Mn(EHGS). Similarly, when a DMF solution of Mn(EHPG)$^-$ is aged for 2 weeks in the presence of dioxygen, a new reductive wave appears at −231 mV in this solvent. An authentic sample of Mn(SALEN)$^+$ shows a reductive wave at −231 mV in DMF. Thus, we conclude that two successive oxidative decarboxylations of Mn(EHPG)$^-$ and Mn(EHGS) occur in methanol and DMF in the presence of dioxygen. In methanol, the decarboxylation of Mn(EHGS) is fast or at least of a comparable rate relative to the decarboxylation of Mn(EHPG)$^-$ since an appreciable concentration of the Mn(EHGS) cannot be detected.

(33) Li, X.; Kessissoglou, D. P.; Kirk, M. L.; Bender, C. J.; Pecoraro, V. L. *Inorg. Chem.* **1988**, *27*, 1.
(34) Kessissoglou, D. P.; Butler, W. M.; Pecoraro, V. L. *Inorg. Chem.* **1986**, *25*, 495.
(35) Kessissoglou, D. P.; Kirk, M. L.; Lah, M. S.; Bender, C.; Pecoraro, V. L. *J. Chem. Soc., Chem. Commun.* **1989**, 84.
(36) Vincent, J. B.; Folting, K.; Huffman, J. C.; Christou, G. *Inorg. Chem.* **1986**, *25*, 996.
(37) Boucher, L. J. *J. Inorg. Nucl. Chem.* **1974**, *36*, 531.

(38) Rotating-platinum-electrode (RPE) voltammetry samples the properties of the bulk solution since the product of the electrode reaction is continuously swept away. This allows one to establish whether an oxidative or reductive current is passed. In contrast, cyclic voltammetry samples the electroactive species at the electrode surface and does not distinguish a priori whether the original state of the electroactive component was oxidized or reduced. For more details see: Bard, A. J.; Faulkner, L. R. *Electrochemical Methods: Fundamentals and Applications*; Wiley: New York, 1980.

Table V. NMR Assignments for Mn(EHPG)$^-$ and Related Complexes

compd	solvent	resonances[a]
rac-Mn(EHPG)$^-$	MeOH	+26.3, −18.6, −34.6
	DMF	+25.2, −17.0, −33.5
meso-Mn(EHPG)$^-$	MeOH	+27.8, +24.0, −2.4, −16.5, −22.5, −32.5, −35.5
	DMF	+27.3, +24.8, −18.0, −21.6, −32.0, −37.7
Mn(EHGS)	DMF	+45.6, +28.6, +13.1, −9.4, −19.5, −27.7
Mn(SALEN)$^+$	MeOH	−4.1, −23.2, −28.9
	DMF	+29.5, −2.4, −22.3, −25.4
Mn(5-Cl-SALEN)$^+$	MeOH	−3.3, −24.5
	DMF	slightly soluble
Mn(3,5-Cl_2-SALEN)$^+$	MeOH	−3.1, −21.6
	DMF	slightly soluble
Mn(4-OMe-SALEN)$^+$	MeOH	−9.48, −19.78
	DMF	+17.52, −5.26, −21.19
Mn(6-OMe-SALEN)$^+$	MeOH	−22.12, −32.29
	DMF	+13.86, −21.94, −25.97

[a] Shifts reported in parts per million relative to TMS = 0 ppm with use of the major solvent resonances in methanol and DMF as internal standards.

This scenario is supported by the bulk oxidation of Mn(EHPG)$^-$ in methanol. When Mn(EHPG)$^-$ is oxidized at +600 mV, 4 equiv of electrons per manganese ion are passed. The resulting CV and RPE are diagnostic of Mn(SALEN)$^+$. Similar oxidative chemistry is observed in DMF with an electrolysis potential of +500 mV. We examined the cyclic voltammetry of Ga(EHPG)$^-$ and the free-base form of EHPG^{4-} to establish whether the observed electrochemistry is primarily metal- or ligand-centered. Gallium(III) is not redox active, has the same charge as Mn(III), and also forms a six-coordinate structure with EHPG.[21] A single, irreversible, ligand-centered oxidation wave is seen at +1038 mV. This potential is over 500 mV more positive than the metal-centered oxidation of Mn(EHPG)$^-$. The free-base form of the ligand is irreversibly oxidized at +760 mV in DMF. Thus, the data reported in Table IV lead to two conclusions. First, the Mn(EHPG)$^-$ oxidation at +453 mV is a metal-centered redox process. This is established since redox-inert M^{III}(EHPG)$^-$ complexes do now show oxidative chemistry in the +100 to +800 mV range. Second, only those metals that are competent to carry out two-electron redox chemistry (e.g., Mn(IV) to Mn(II) or V(V) to V(III)) will induce the oxidative decarboxylation of the ligand.

Paramagnetic NMR Studies. In a previous report,[39] we have shown that monitoring the isotropically shifted proton resonances of Mn(III) phenolates provides useful information for understanding solution speciation and dimerization processes. In this contribution, we provide the first example of how paramagnetic NMR spectroscopy is a sensitive tool for following the chemical reactions of Mn(III) phenolate complexes. NMR shifts are provided in Table V. Figure 5 shows the paramagnetic NMR spectra of different isomers of MnEHPG$^-$ and proton NMR spectra of their corresponding ligands. Figure 5C illustrates the paramagnetic ^{1}H NMR spectrum of *meso*-Mn(EHPG)$^-$ in methanol. The initial spectrum (Figure 5C) shows three sets of two approximately equal intensity resonances at +27.9 and +24.0, −16.5 and −22.5, and −32.5 and −35.5 ppm (referenced to $(CH_3)_4Si$ with downfield shifts taken as positive). In addition, a single sharp resonance is observed at −2.4 ppm. These features are the result of the mechanism of spin delocalization, which gives rise to large chemical shifts for the phenolate protons and the isomeric composition of Mn(EHPG)$^-$. A strong phenolate-to-metal charge-transfer excitation is observed[40] at 354 nm (ϵ = 3630 M^{-1} cm^{-1}) for Mn(EHPG)$^-$. For metals of the appropriate electronic spin relaxation time, the chemical shift pattern of $|\delta(o\text{-H})| > |\delta(m\text{-H})| > |\delta(p\text{-H})|$ with alternating upfield and downfield shifts is observed when spin delocalization into a π molecular orbital system occurs primarily via a scalar mechanism.[41-44] Such a pattern is observed[41] for Fe(SALEN)X (e.g., Fe(SALEN)Cl shows the following: 4-H, +79.1 ppm; 5-H, −67.9 ppm; 6-H, +49.7 ppm). As shown in Figure 5A, a similar pattern of alternating upfield and downfield resonances is observed for Mn(EHPG)$^-$. Thus, we would expect the pairs of resonances to be assigned as follows: −34.6 and −37.6 (4-H); +22.3 and +26.3 (5-H); −18.6 and −24.6 (6-H). The sharp feature at −2.4 ppm is most likely due to the α-C proton. The reversal of the sign of the chemical shift is probably due to the transfer of upspin to the high-spin, d^4 Mn(III) rather than downspin to the high-spin, d^5 Fe(III).

One result of the diastereomeric nature of metallo EHPG complexes is that the physical properties of each isomer are, in theory, distinguishable. Thus, one might be able to assign resonances in the NMR spectra to different coordination isomers. Commercial samples of H_4EHPG are composed of a 60:40 mixture of *rac* and *meso* isomers (determined by the integrated intensity of the α-C proton resonances). From this mixture, four diastereomeric pairs of isomers can be generated. We isolated pure *rac*-Mn^{III}(EHPG)$^-$ and *meso*-Mn^{III}(EHPG)$^-$ complexes in order to determine whether the pairs of resonances were due to the different isomers. It was previously shown that, in methanol, the *meso* isomer of the vanadium EHPG species rapidly decarboxylates to form VO(SALEN), while the *rac* isomer undergoes metal hydrolysis to form the stable pervanadyl EHPG species. Therefore, *rac*-Mn^{III}(EHPG)$^-$ was prepared by demetalation of this *rac*-VO_2(EHPG)$^{3-}$ with use of acid, followed by direct reaction of the isolated ligand with manganese(III) acetate as described in the Experimental Section. The NMR spectrum of this complex in methanol-d_4 is shown in Figure 5A. The ^{1}H NMR spectrum of the uncomplexed ligand is provided adjacent to this spectrum. It is obvious that the resonances associated with the *rac* isomer (Figure 5A, Table V) were not seen in the previous samples (Figure 5C). Therefore, we reinvestigated the composition of the isolated Mn(EHPG)$^-$. One can extract Mn(III) from EHPG^{4-} using 8-hydroxyquinoline. The ^{1}H NMR spectrum of the resulting uncomplexed ligand definitively demonstrates that the originally isolated material contained exclusively the *meso*-Mn(EHPG)$^-$ isomers. Figure 5B illustrates the ^{1}H NMR spectrum obtained for an ~50:50 mixture of *rac*- and *meso*-Mn(EHPG)$^-$ isomers and the corresponding spectrum of the uncomplexed ligand mixture. We conclude from these data that the paramagnetic NMR spectra are sufficiently sensitive to distinguish the different stereochemical isomers of Mn(EHPG)$^-$.

There are two possible reasons that the spectrum of the *meso* isomer shows three pairs of resonances while the *rac* isomer exhibits only one set of three peaks. First, potentiometric titrations have shown that *rac*-Λ-(*RR*)-Fe(EHPG)$^-$ (or the Δ-(*SS*) isomer) is 2 orders of magnitude more stable than the corresponding *meso* isomers.[30] A stereochemical analysis[21] attributed this to the preferred trans carboxylate configuration of the *rac*-Λ-*RR* (or *rac*-Δ-*SS*) compared to the all-cis configuration for the *meso* isomers. The *rac*-Λ-*SS*/*rac*-Δ-*RR* isomer is expected to be even more destabilized, since this requires trans imino phenolate coordination (see Figure 2). This preference would be exacerbated by the Jahn–Teller distortion of the Mn(III) ion. Thus, one expects less than 1% of *rac*-Mn(EHPG)$^-$ to be in the trans-phenolate (Δ-*RR*/Λ-*SS*) configuration and one should see resonances due solely to the *rac*-Λ-*RR* (or Δ-*SS*) complex. In contrast, there is little thermodynamic difference between the Λ-*SR* (Δ-*RS*) and Λ-*RS* (Δ-*SR*) configurations so that roughly equal mixtures

(39) Bonadies, J. A.; Maroney, M. J.; Pecoraro, V. L. *Inorg. Chem.* **1989**, *28*, 2044.
(40) Patch, M. G.; Carrano, C. J. *Inorg. Chim. Acta* **1981**, *56*, L71.
(41) Pyrz, J. W.; Roe, A. L.; Stern, L. J.; Que, L., Jr. *J. Am. Chem. Soc.* **1985**, *107*, 614.
(42) LaMar, G. N.; Eaton, G. R.; Holm, R. H.; Walker, F. A. *J. Am. Chem. Soc.* **1973**, *95*, 63.
(43) Heistand, R. H., II; Lauffer, R. B.; Fikrig, E.; Que, L., Jr. *J. Am. Chem. Soc.* **1982**, *104*, 2789.
(44) LaMar, G. N. In *NMR of Paramagnetic Molecules: Principles and Applications*; LaMar, G. N., Horrocks, W. D., Holm, R. H., Eds.; Academic Press: New York, 1973; Chapter 3. Horrocks, W. D., Jr. *Ibid.*, Chapter 4.

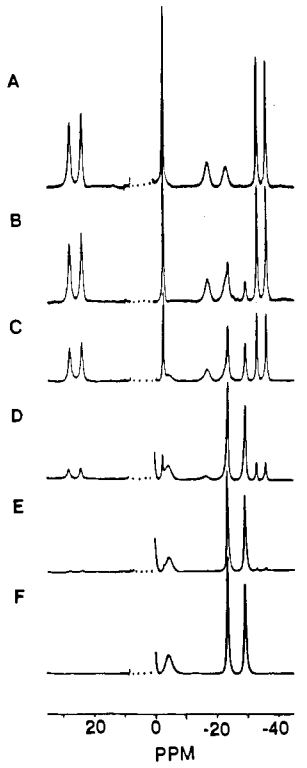

Figure 6. ^{1}H NMR spectra of an approximately 10 mM methanol-d_4 solution of Mn(EHPG)$^-$ at varying time periods: (A) initial; (B) 2 days; (C) 4 days; (D) 6 days; (E) 9 days. Spectrum F is that of Mn(SALEN)$^+$.

of the two *meso* isomers are predicted. This is seen in Figure 5C. Alternatively, the two sets of phenolate resonances could result from a slightly different extent of charge transfer from phenolates that are trans to an amine versus those trans to a carboxylate. In the preferred *rac* isomer, both phenolates are trans to the amine nitrogen, while in the *meso* isomers, one phenolate is trans to an amine and the other phenolate is trans to a carboxylate moiety. Therefore, both models can explain our results. However, we prefer the first description since the peaks at +24.0, −16.5, and −32.5 ppm have slightly greater intensity than those at +27.8, −22.5, and −35.5 ppm. This difference could easily be explained by a small thermodynamic preference for one of the *meso* isomers, while one must invoke a difference in charge-transfer efficiency based on trans ligation to explain these relative intensities using the latter model.

Having assigned the features of the parent Mn(EHPG)$^-$ spectrum, we investigated the Mn(EHPG)$^-$ decarboxylation in methanol-d_4 as illustrated in Figure 6. The progressive loss of features associated with Mn(EHPG)$^-$ is observed over the course of 9 days. These are replaced by new resonances at −4.1, −23.2, and −28.9 ppm. These peaks can be assigned to the Mn(SALEN)$^+$ cation on the basis of the spectrum of authentic Mn(SALEN)$^+$ shown at the bottom of Figure 6. As we have shown previously,[39] all of these peaks arise from the phenolate protons of SALEN. However, unlike the case for Mn(EHPG)$^-$, the simple π-delocalization model is no longer an appropriate description. We believe that this is due to spin delocalization onto the phenyl ring via two independent paths. These are the phenolate oxygen atom and the conjugated imine nitrogen atom. Nonscalar terms may also cause marked deviations from the simple π-delocalization model, since Mn(III) has a ^{5}E ground state (octahedral assumption), which may lead to an anisotropic **g** tensor. Furthermore, both up- and downspin can be transferred with Mn(III) while only downspin can be transferred with Fe(III). The data for the ring-substituted derivatives provided in Table V allow us to assign the Mn(SALEN)$^+$ resonances as −4.1 (6-H), −23.2 (5-H), and −28.9 (4-H). Because of the poor solubility of the substituted derivatives in DMF we were unable to make the corresponding assignments in this solvent; however, it is most likely

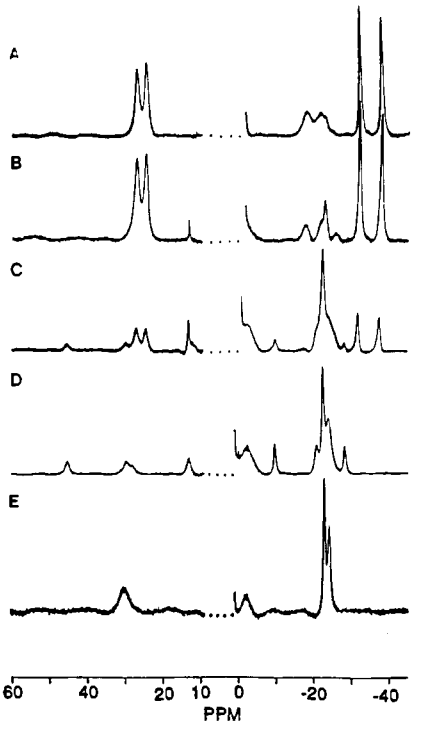

Figure 7. NMR spectra of an approximately 10 mM DMF solution of Mn(EHPG)$^-$ at varying time periods: (A) initial; (B) 7 h; (C) 3 days; (D) 8 days. Spectrum E is that of Mn(SALEN)$^+$.

Scheme I

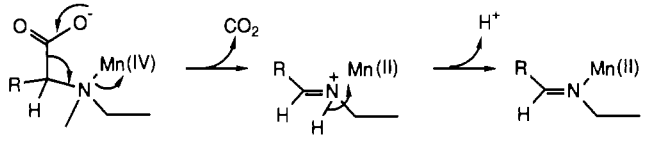

that the far-upfield resonances once again are a result of the ring 4- and 5-protons. These data are consistent with our previous assignment[39] of protons with Mn(2-OH-SALPN)$^+$.

The spectra in Figure 6 provide no evidence for the formation of an Mn(EHGS) intermediate. In contrast, the decarboxylation of Mn(EHPG)$^-$ in DMF, illustrated in Figure 7, clearly shows features after 3 days that cannot be attributed to either Mn(EHPG)$^-$ (top) or Mn(SALEN)$^+$ (bottom). The resonances at +45.6, +28.6, +13.1, −9.4, −19.5, and −27.7 ppm are assigned to Mn(EHGS). There are many more features for Mn(EHGS) than for either Mn(EHPG)$^-$ or Mn(SALEN)$^+$ because the monodecarboxylated derivative contains resonances from both phenolate and imino phenolate type protons. The simple phenolate protons are expected to behave somewhat like those of Mn(EHPG)$^-$ (alternating upfield/downfield shifts), while the imino phenolate protons would be more similar to those of Mn(SALEN)$^+$ (exclusively upfield shifts). We have not attempted to assign the features of the Mn(EHGS) spectrum due to its complexity and the instability of the complex; however, the NMR spectra in Figure 7 support the formation of this intermediate, monodecarboxylated complex in DMF. After 10 days Mn(SALEN)$^+$ is the sole product.

Proposed Mechanism of Decarboxylation. Scheme I illustrates one possible chemical mechanism that requires a two-electron, metal-centered reduction during the process, and Figure 8 shows the proposed stepwise nature of the decarboxylation of Mn(EHPG)$^-$. Addition of dioxygen to an Mn(EHPG)$^-$ solution initially results in the neutral Mn(IV) compound Mn(EHPG). This molecule undergoes a two-electron oxidation across the carbon–nitrogen bond, generating 1 equiv each of CO_2, H^+, and Mn^{II}(EHGS)$^-$. This metal complex is very air sensitive and will rapidly form the analogous Mn^{IV}(EHGS)$^+$, which is oxidatively unstable to the formation of CO_2, H^+, and Mn^{II}(SALEN). The isolated product is Mn^{III}(SALEN)X.

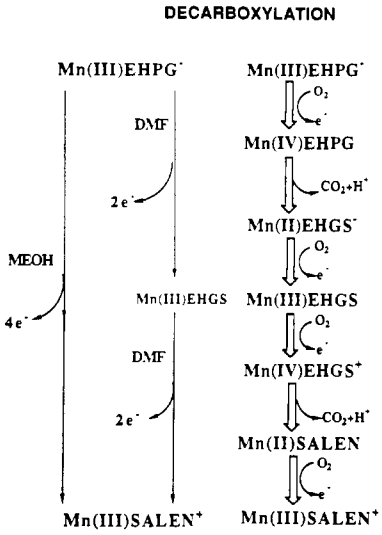

Figure 8. Proposed mechanism for oxidative decarboxylation of Mn(EHPG)⁻ and Mn(EHGS). This scheme follows the previously reported decarboxylation of VO(HEHPG).

The stoichiometric mechanism shown here is analogous to that reported[16,17] for the oxidative decarboxylation of VO(HEHPG). In the vanadium system, crystals of the V(IV) intermediate VO(EHGS)⁻ were isolated and characterized.[45] That manganese follows this reactivity pathway is supported by the following observations. Under nitrogen, $Mn^{III}(EHPG)^-$ is indefinitely stable in methanol, DMF, or acetone. Addition of dioxygen to these solutions results in the isolation of Mn(SALEN)X. Similar results are obtained by bulk oxidations of $Mn^{III}(EHPG)^-$ in methanol at ~+600 mV. Cyclic and rotating-platinum-disk voltammetries showed that a one-electron oxidation occurred at potentials that were less positive than the electrolysis potential. These electrolyses consumed the requisite number of electrons (four) for complete reaction by this model. $Ga^{III}(EHPG)^-$ showed a ligand-centered oxidaton only at potentials greater than +1 V, indicating that the electrochemistry of the manganese compounds is initially metal centered. The paramagnetic NMR spectra show a clean conversion of $Mn^{III}(EHPG)^-$ to $Mn^{III}(SALEN)^+$ in methanol; however, DMF solutions develop resonances that are assigned to the monodecarboxylated ligand complex Mn(EHGS). Unlike the manganese and vanadium materials, $Ga^{III}(EHPG)^-$, $Fe^{III}(EHPG)^-$, and $Cu^{II}(EHPG)^{2-}$ are stable indefinitely under aerobic conditions. We believe this is due to the relative inaccessibility of higher oxidation state complexes (e.g., Fe(IV)) with these ligands.

Conclusions. This report demonstrates that, under certain circumstances, the reactivity patterns of mononuclear manganese complexes more closely mimic vanadium rather than iron. This is because of the three easily accessible oxidation states for Mn (II, III, IV) and vanadium (III, IV, V), while two oxidation states dominate iron chemistry (II, III) with amino polycarboxylate ligands. An important distinction between vanadium and manganese is the relative oxophilicity of the high-valent ions. Vanadium(V) is found as either the monooxo or *cis*-dioxo complex, and vanadium(IV) usually occurs as the vanadyl ion. Only as Mn(V), Mn(VI), or Mn(VII) are manganyl ions important contributors to the chemistry. This implies that manganese may be a useful two-electron oxidant using specifically tailored, redox-inert ligands, forming Mn(IV) complexes that are coordinatively unsaturated.

At this point, it is useful to put the observations of the EHPG system in perspective with the known biological roles for manganese. Manganese superoxide dismutase catalyzes one-electron-redox chemistry exclusively. Thus, superoxide is a substrate for this enzyme while hydrogen peroxide is not.[3] In contrast, the dinuclear manganese catalase of *L. plantarum* facilitates two-electron reactions but will not act as a superoxide dismutase.[2] Manganese would appear to donate one electron per metal center in these systems. Similarly, four electrons are required for water oxidation in the photosynthetic oxygen-evolving complex, which contains four manganese ions. Thus, all of the manganese-associated biological processes so far discovered occur via an average one electron per metal stoichiometry, although it has as yet not been proved that every metal center in these proteins is redox active.

Finally, the occurrence of carboxylate residues at the active site of a manganoenzyme that requires the Mn(IV) oxidation level for catalysis should not be ruled out on the basis of the observed decarboxylation reactions of $MnEHPG^-$ or MnEHGS. The proximity of the acidic proton on the amine nitrogen and the stability of the resulting SALEN molecule facilitate the decarboxylation reaction. An amino acid side chain positions a methylene group adjacent to the carboxylate. This configuration should be much more stable toward the oxidative chemistry described herein.

Acknowledgment. We wish to thank Dr. J. A. Bonadies and Prof. M. Maroney for useful discussions and Dr. W. M. Butler for the X-ray structure determination. This research was supported by the NIH (Grant No. GM-39406). V.L.P. thanks the G. D. Searle Family and Chicago Community Trust for a Biomedical Research Scholar Award (1986–1989) and the Alfred P. Sloan Foundation for a fellowship (1989–1991).

Supplementary Material Available: Tables VI–IX, providing anisotropic thermal parameters of all non-hydrogen atoms, fractional atomic positions for hydrogen atoms, a complete set of bond distances, and a complete set of bond angles for **5**, respectively, and Figure 9, providing a complete numbering scheme for all atoms (6 pages); Table X, providing observed and calculated structure factors (8 pages). Ordering information is given on any current masthead page.

(45) Riley, P. E.; Pecoraro, V. L.; Bonadies, J. A.; Carrano, C. J.; Raymond, K. N. *Inorg. Chem.* **1986**, *25*, 154.